

## Sb(III) as a Surface Site for Water Adsorption on Sn(Sb)O<sub>2</sub>, and Its Effect on Catalytic Activity and Sensor Behavior

Vincent Dusastre and David E. Williams\*

Chemistry Department, University College London, 20 Gordon Street, WC1H 0AJ, UK

Received: March 5, 1998; In Final Form: June 3, 1998

Surface segregation of Sb in polycrystalline Sn(Sb)O<sub>2</sub> is known to affect the rate of surface-catalyzed combustion of hydrocarbons and carbon monoxide over this material. This combustion rate is also known to be affected by the presence of water vapor. We show that Sb segregation to the surface as Sb(III) in Sn<sub>1-x</sub>Sb<sub>x</sub>O<sub>2</sub> ( $x = 0.005, 0.05$ ), controllable by thermal treatment, strongly alters the effect of water vapor both upon the surface-catalyzed combustion rate of carbon monoxide and upon the elevated-temperature electrical conductivity. We suggest that the surface defect states which mediate both the electrical behavior and the surface-catalyzed combustion are best formulated as an association complex of an oxygen vacancy with Sn(II) or Sb(III), and are then able to propose a simple model which unifies the interpretation of the behavior of SnO<sub>2</sub> as both a gas sensor and a combustion catalyst. We postulate: that a correct formulation of the “adsorbed oxygen” (O<sup>2-</sup>) surface species mediating the electrical response is an oxygen molecule trapped in or on a surface oxygen vacancy; that the combustion reaction proceeds partly through these species and partly through lattice oxygen at the surface; that water competes with oxygen for the surface vacancies, blocking this route; and that the binding energy of water to the Sb(III)·V<sub>O</sub> surface defect complex is less than that to the Sn(II)·V<sub>O</sub> complex.

### Introduction

Antimony–tin oxide catalysts are well-known to be active and selective for olefin oxidation, oxidative dehydrogenation, and ammoxidation of alkenes, notably propylene to acrolein and acrylonitrile,<sup>1–3</sup> and have previously been developed for the selective oxidation of hydrocarbons (methane<sup>4</sup>). The behavior contrasts with that of pure SnO<sub>2</sub>, which favors deep oxidation.<sup>5,6</sup> Optimal catalytic activity is obtained with fairly large antimony concentrations (~30% Sb cations<sup>1</sup>). Although Sb substitution appears to occur without strong modification of the SnO<sub>2</sub> lattice, the reported solubility limit of antimony cations in the rutile phase of SnO<sub>2</sub>, from structural studies, varies from 3<sup>7</sup> to 40%.<sup>8</sup> The catalytic performance of these compounds depends critically upon the conditions of preparation and particularly upon the calcination temperature adopted. These conditions have been reported<sup>9,10</sup> to have an effect on the properties of the materials, such as the surface area, the particle size, and the surface composition. The surface composition of these oxides varies from the bulk composition. There is, especially, surface enrichment in antimony which takes place to an extent dependent upon bulk composition and calcination temperature. Pronounced enrichment by antimony at the surface was observed by X-ray photoelectron spectroscopy (XPS) with a heat of segregation varying from roughly 10 (40 at. % Sb) to 40 (0.5 at. % Sb) kJ/mol.<sup>11</sup> Comparison of the influence of calcination temperature upon surface composition (by XPS) with the effect upon bulk phase composition (X-ray diffraction study) has shown<sup>9,12</sup> a region which contains a Sb<sub>2</sub>O<sub>4</sub> surface phase which appears at high temperature and which exhibits decreasing surface antimony composition with increasing temperature as a consequence of vaporization of Sb<sub>2</sub>O<sub>4</sub>.

Cross and Pyke<sup>11</sup> studied Sb segregation upon calcination of oxides prepared by a coprecipitation method. As water was

lost from the hydrous oxide, the onset of antimony surface enrichment at 400 °C corresponded exactly to a change in color from white to deep blue, which the authors interpreted as being due to antimony lattice diffusion and reconstruction. At 600 °C, by analogy with (NH<sub>4</sub>)<sub>2</sub>SbBr<sub>6</sub>,<sup>13</sup> the color change is possibly due to charge transfer between Sb<sup>3+</sup> and Sb<sup>5+</sup> within a random array of disordered SnO<sub>6</sub> and SbO<sub>6</sub> octahedra.<sup>7</sup> The results are therefore consistent with the prediction that catalyst preparation forces antimony into an environment in which it is not particularly stable, so that at high temperatures segregation to surfaces takes place where antimony could occupy an energetically more favorable situation, probably as Sb<sup>3+</sup>.<sup>14,15</sup>

SnO<sub>2</sub> is a semiconductor with a direct band gap of 3.6 eV between the full oxygen 2p valence band and the tin states at the bottom of the conduction band. The electronic conduction of stannic oxide has been attributed to oxygen vacancy donor levels and can be enhanced by reduction.<sup>16</sup> Introducing carriers in SnO<sub>2</sub> by antimony doping results in a dramatic increase in the electrical conductivity because of substitution of Sb(V) into the SnO<sub>2</sub> lattice.<sup>17,18</sup> Model calculations compared with infrared reflectance measurements for various Sb doping levels suggested, however, that for doping levels > 1 at. %, the sample might be covered with a reduced carrier concentration surface layer, consistent with Sb segregation to the surface as Sb(III).<sup>19</sup>

Catalytic reaction between reducing species and surface-adsorbed oxygen at elevated temperatures releases carriers in the tin dioxide conduction band. Changes in conductivity of tin dioxide associated with the interaction with reducing gases provide the basis for application of these systems as gas sensors.<sup>20</sup> The electrical conductivity is, in fact, a very sensitive probe of the surface state of the oxide. Semiconductor gas detectors are sensitive to water vapor and their response to combustible gases is affected by the ambient humidity.<sup>21,22</sup> Thus, it has been observed that water adsorbs in greater quantities

than oxygen on the surface of tin dioxide.<sup>23</sup> Water is strongly bound to an SnO<sub>2</sub> surface, possibly as surface Sn–OH groups. On heating, minor water loss is observed at 373 K, the major loss taking place in the range 520–720 K. The effect of moisture on gas sensitivity has been discussed<sup>24</sup> in terms of the displacement of chemisorbed oxygen by H<sub>2</sub>O and OH<sup>-</sup>. On SnO<sub>2</sub> the chemisorption of water seems to introduce a surface electronic state such as a surface hydroxyl species.<sup>24</sup> Recently, the presence of dissociatively adsorbed water on SnO<sub>2</sub>(110) has been observed using a combination of ultraviolet photoelectron spectroscopy (UPS) and temperature-programmed desorption spectroscopy (TPDS).<sup>25</sup> In these studies, H<sub>2</sub>O acts as an electron donor, bending the bands down at the surface and increasing the surface carrier concentration. The increase in surface conductivity caused by H<sub>2</sub>O is greater on slightly reduced surfaces than on heavily reduced, disordered ones.<sup>26</sup>

The behavior of Sb-doped tin dioxide as a gas sensor material has been extensively reported. However, there has been little or no investigation of the effect of antimony enrichment at the surface as Sb(III) on either adsorption, catalysis, or gas sensor behavior, despite the speculation by Egdell et al.<sup>27</sup> that there should be an interaction of Sb(III) surface species with molecules which can act as electron acceptors. In the present paper, we show that the surface segregation of Sb in polycrystalline Sb-doped SnO<sub>2</sub> can be controlled by an appropriate preparation regime. We confirm earlier XPS observations implying the presence of Sb(III) at the surface and correlate this with the measurements of surface segregation. By measuring the electrical behavior in response to exposure to water vapor in air at elevated temperature we then deduce the existence of an electrically active surface state associated with preferential water adsorption on Sb(III), thereby supporting earlier speculation concerning the significance of this state.<sup>27,28</sup> Finally, we demonstrate an effect of Sb(III) segregation on oxidation catalysis. The effect is found only in the presence of water vapor. We propose a connection between the electrical properties and the catalytic activity which rationalizes the results.

## Experimental Section

The oxides Sn<sub>1-y</sub>Sb<sub>y</sub>O<sub>2</sub> ( $y = 0, 0.005, 0.05$ ) were prepared by coprecipitation<sup>7</sup> using the following procedure. Weighed amounts of antimony (Ventron, purity > 99.999%) and tin (Fluka, purity > 99.999%) were dissolved in aqua regia. An excess of NH<sub>3</sub> was added to the solution to make it alkaline. After the mixture boiled for a few hours, the resulting precipitate was washed and collected. After the precipitate dried overnight at 120 °C, the powdered materials were fired for 12 h at different temperatures (600, 800, 1000, and 1200 °C) in air in recrystallized alumina crucibles. The coprecipitated materials were white in color after drying at 120 °C, and became blue on heating to 600 °C. The blue color darkened with increasing firing temperature. The materials were then ground, pressed at 1 ton into 13 mm diameter 1.5 mm thick pellets and fired at the same temperature as the initial firing for 12 h.

The electrical behavior of the pellets under controlled humidity and temperature conditions was monitored in a computer-controlled rig (described in ref 29). Two-terminal dc resistance measurements were employed, the accuracy of these measurements having been independently cross-checked against ac measurements. Water vapor pressure was controlled by mixing dry gas with gas that had been saturated with water vapor by passing through a bubbler.

X-ray powder diffractometry (Siemens D5000, transmission mode with incident beam monochromator and Cu K $\alpha$  radiation)

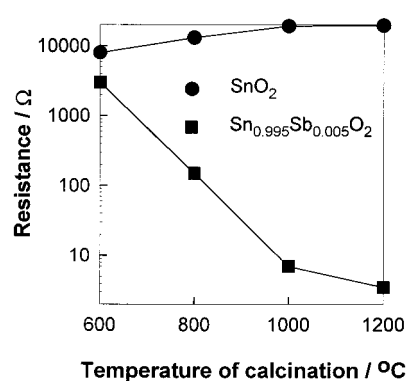


**Figure 1.** Electrical resistivity of Sn<sub>1-y</sub>Sb<sub>y</sub>O<sub>2</sub> porous pellets exposed to dry air at 400 °C, as a function of calcination temperature.

showed the presence of a single well-crystallized rutile phase, whose lattice parameters were the same as those of undoped SnO<sub>2</sub>. The average crystallite size, determined from the diffraction line width and cross-checked by scanning electron microscopy and surface area measurement, increased smoothly with calcination temperature from roughly 25 (600 °C; consistent with ref 7) to 150 nm (1200 °C) for 0.5% Sb-doped materials. XPS spectra were recorded (VG ESCALAB 220iXL instrument) using focused (300  $\mu$ m spot size) monochromatized Al K $\alpha$  radiation. The binding energies were referenced to the hydrocarbon C 1s peak at 284.80 eV and the sample charging was controlled with a 3 eV flood gun. Spectrum quantification and curve fitting was performed using a Shirley background and sensitivity factors were obtained from Wagner et al.<sup>30</sup>

Gas combustion measurements were performed with a quartz reactor tube (15 mm in diameter) and quartz frit upon which 1 g of the powder was placed. The reacting gases (1000 ppm in 21% O<sub>2</sub>, 79% N<sub>2</sub>, or Ar) were supplied at 50 cm<sup>3</sup>min<sup>-1</sup> through mass-flow controllers (Tylan) to the reactor tube mounted vertically in a tube furnace. The temperature was ramped from 25 to 600 °C at 10 °C·min<sup>-1</sup>. A quadrupole mass spectrometer was used to measure the concentrations in the gas stream after passage through the reaction tube. For CO oxidation the gas mixtures contained Ar instead of N<sub>2</sub> to remove the mass 28 interference. Carbon dioxide was the only product detected. The mass spectrometer signal was linear in concentration of CO, CH<sub>4</sub>, and CO<sub>2</sub>. The pseudo-first-order rate constant for the surface-catalyzed combustion was calculated as previously described.<sup>31</sup> Specific surface area was determined by krypton adsorption at 77 K using a volumetric procedure. Values very similar to those noted by Brown and Patterson<sup>4</sup> were obtained. For comparison of materials, the rate constant was normalized by the surface area of the sample.

## Results

**Sb Surface Segregation.** The variation of electrical conductivity with calcination temperature is shown in Figure 1. The material calcined at 600 °C had properties essentially the same as those of the undoped SnO<sub>2</sub> calcined at the same temperature, and it must be concluded that this material was unreacted. Such a material has been described as an unordered assembly of Sb- and Sn-centered octahedra.<sup>4,7</sup> The variation of conductivity with reaction temperature could, in absence of other information, be taken simply to illustrate the variation in degree of reaction with calcination temperature. However, XPS demonstrates that the effect is related to the temperature-dependent surface segregation of Sb. Al K $\alpha$  excited photoelectron spectra in the region O1s and Sb3d are shown in Figure 2. The Sb 3d<sub>5/2</sub> peak overlaps

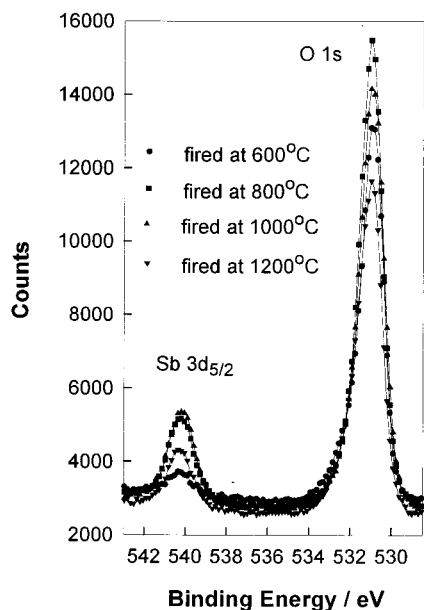


**Figure 2.** Photoelectron spectra of the O 1s and Sb 3d region for  $\text{Sn}_{0.995}\text{Sb}_{0.005}\text{O}_2$  materials calcined at different temperature.

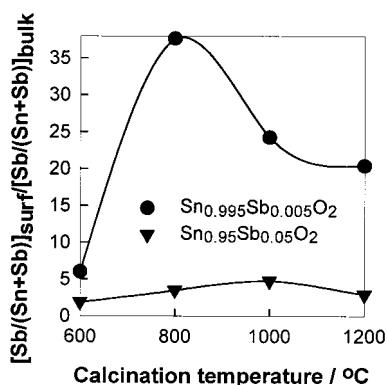


**Figure 3.** Variation of surface composition with calcination temperature at constant bulk concentration and calcination period (12 h).

with the O1s peak, but from the intensity and assuming the  $\text{Sb}3d_{3/2}/\text{Sb}3d_{5/2}$  intensity ratio, the atomic percent of Sb segregation could be calculated. Variation of the calcination temperature produced systematic changes in surface composition determined from XPS data (Figure 3). The surface enrichment factor was observed to vary dramatically with bulk composition (by a factor of 10 between 0.5 and 5% Sb-doped compounds at 800 °C) at constant calcination temperature. Both series of doped materials (0.5 and 5% Sb) exhibited a firing temperature of maximum Sb enrichment, the maximum shifting to higher temperature (1000 °C instead of 800 °C) at higher antimony concentration. If the effect were simply due to a variation in degree of reaction, then a monotonic variation of Sb signal with calcination temperature would be expected, rather than the observed maximum. The enhancement in segregation with decrease of temperature corresponds to a heat of segregation  $\Delta H_{\text{seg}} \approx -20 \text{ kJ mole}^{-1}$ , consistent with the results in ref 11.

XPS and UPS study of conduction electrons in Sb-implanted  $\text{SnO}_2$  films showed<sup>32</sup> that not all of the implanted Sb ions on the surface acted as donor centers but that some behaved as trapping centers. The mechanism for carrier trapping was explained by consideration of photoemission structure in the band gap region between the valence band (VB) and the conduction band (CB).<sup>33</sup> The significant structure was a small shoulder at the valence band edge of the pure  $\text{SnO}_2$ , which was

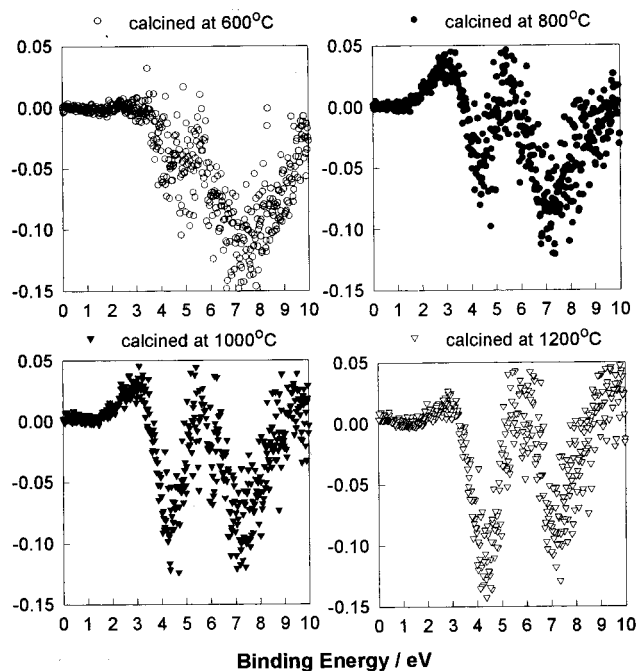


**Figure 4.** Photoemission difference spectra (undoped  $\text{SnO}_2$  - 0.5% Sb doped  $\text{SnO}_2$ ) for materials calcined at different temperature. The spectra were normalized to the intensity of the valence band maximum.

removed by Sb implantation. Photoemission difference spectra (Sb-implanted - pure  $\text{SnO}_2$ ) were used to display this effect clearly. Our XPS measurements in the valence band region confirmed this effect for the polycrystalline powder material and showed its correlation with Sb segregation (see Figure 4). Materials fired at 800 °C which correspond to the highest Sb segregation showed a significant difference peak at 3 eV binding energy. This difference peak did not appear for materials calcined at 600 °C, confirming the interpretation that this material comprised a random array of disordered  $\text{SnO}_6$  and  $\text{SbO}_6$  octahedra,<sup>7</sup> rather than a solid solution of Sb in  $\text{SnO}_2$ . For materials calcined at higher temperature the difference peak intensity correlated with the surface segregation, being greatest for largest surface Sb concentration. As noted in ref 33, the difference spectrum at higher binding energy is dominated by a shift to higher binding energy of the main O 2p valence band structure (higher binding energy in the doped material). For these polycrystalline, untextured materials, the difference spectrum implies that Sb doping also causes a broadening of this peak as well as a shift.

**Elevated-Temperature Electrical Response to Changing Water Vapor Pressure.** The sensitivity of the electrical conductivity to variations of water vapor pressure ( $S_{\text{H}_2\text{O}}$ ) is defined as  $S_{\text{H}_2\text{O}} = (R_{\text{dry}} - R_{\text{wet}})/R_{\text{wet}}$ . The sensitivity to water as a function of partial pressure of the gas at 25 °C, determined at 400 °C increased roughly linearly with the partial pressure and decreased significantly with the antimony doping. Whereas for undoped materials the sensitivity decreased monotonically with the increase in crystallite size as the calcination temperature increased, the Sb-doped materials behaved differently, exhibiting an enhanced sensitivity (by a factor of 2) to water at a calcination temperature of 800 °C. These critical measurements were repeated for confirmation. Comparing  $S_{\text{H}_2\text{O}}$  (50% relative humidity (RH) at 20 °C = 1244 Pa) at 400 °C (Figure 5) for undoped and 0.5% Sb-doped materials shows the clear correlation of  $S_{\text{H}_2\text{O}}$  with surface antimony segregation.

**Catalyzed Combustion.** The reaction product of both methane and carbon monoxide (dry and wet) over  $\text{Sn}_{1-\gamma}\text{Sb}_\gamma\text{O}_2$

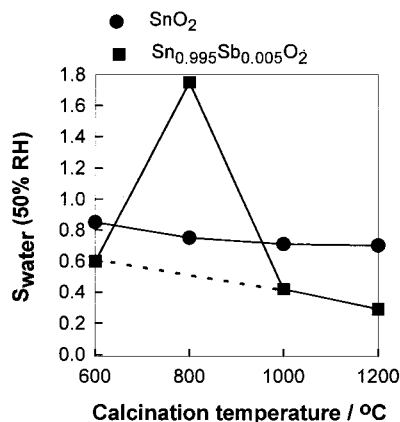


**Figure 5.** Sensitivity,  $S_{\text{water}} = (R_{\text{dry}} - R_{\text{wet}}) / R_{\text{wet}}$  of electrical conductivity to water vapor (1244 Pa  $\equiv$  50% relative humidity at 25 °C) measured at 400 °C, as a function of calcination temperature of  $\text{Sn}_{1-x}\text{Sb}_x\text{O}_2$  porous pellets.

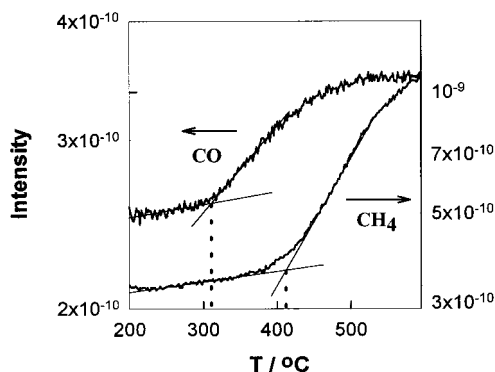


**Figure 6.** Catalytic oxidation of CO and CH<sub>4</sub> in a packed-bed, flow-through reactor: mass 44 ( $\text{CO}_2^+$ ) intensity against reactor temperature for oxidation of 1000 ppm CO and 10000 ppm CH<sub>4</sub> in 21% O<sub>2</sub> + 79% Ar over  $\text{SnO}_2$  calcined at 800 °C.

was carbon dioxide. The reaction of these gases was monitored by looking at the mass 44 intensity as a function of temperature. The onset temperature of methane combustion was around 450 °C for  $\text{SnO}_2$  (Figure 6) and around 500 °C for the antimony-doped samples, and carbon monoxide oxidation occurred at around 300 °C for all of our materials. At 400 °C the mass spectrometry data indicated that 60% of the carbon monoxide and virtually none of the methane had reacted upon passage through the packed bed of the solid. The first-order rate constant for methane combustion, calculated from these data, was approximately 100 times greater than that given by Brown and Patterson,<sup>4</sup> consistent with the 100-times increase in oxygen partial pressure.

Figure 7 represents the variation of the pseudo-first-order rate constant with temperature for surface-catalyzed combustion of dry and wet CO for materials fired at different temperature. The variation with temperature follows an Arrhenius form. The consistency of results for the undoped  $\text{SnO}_2$  indicates a relative error of no more than  $\pm 10\%$  in the rate constant normalized to the surface area. On the undoped  $\text{SnO}_2$ , the effect of introduction of water vapor was to decrease the rate but leave the activation energy unchanged. In dry gas, the rate constant for the Sb-doped materials was identical within experimental error to that of the undoped  $\text{SnO}_2$ . However, in wet gas, the activation energy for combustion catalyzed on the Sb-doped materials was increased to a degree dependent on the calcination temperature. These critical measurements were repeated for confirmation. The activation energy for combustion over all of the materials

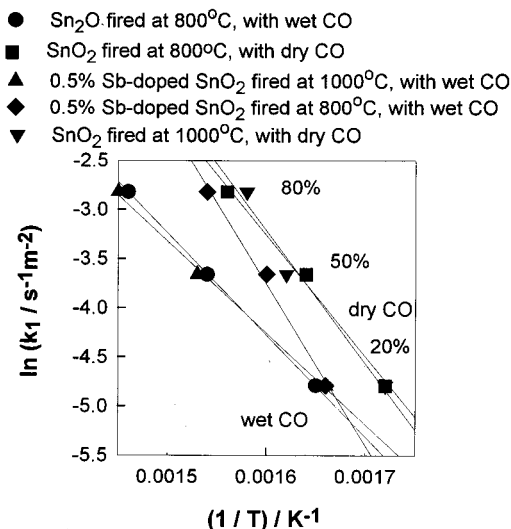


**Figure 7.** First-order rate constant,  $k_1$ , for catalyzed oxidation of CO, against temperature,  $T$ . The labels (20%, 50%, 80%) refer to the degree of conversion of CO to CO<sub>2</sub> on passage through the reactor bed.

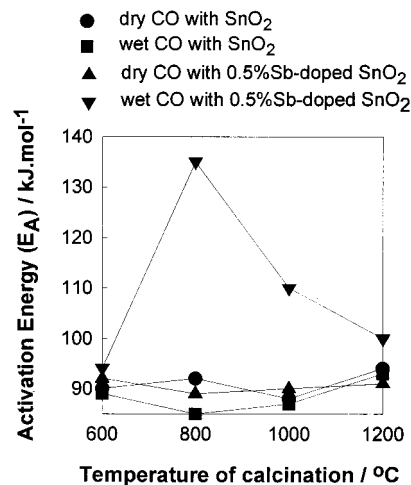


**Figure 8.** Activation energy for CO oxidation in both wet (2500 Pa  $\equiv$  100% relative humidity at room temperature) and dry gas against calcination temperature of the  $\text{Sn}_{1-x}\text{Sb}_x\text{O}_2$  catalyst.

with dry and wet CO is plotted against calcination temperature in Figure 8. A clear maximum, correlating with the temperature-dependent surface segregation of Sb, is shown. The effect of Sb segregation is perhaps better described as causing, over the temperature range of observation, an increase in rate of combustion in wet gas from that characteristic of wet gas on undoped  $\text{SnO}_2$  to that characteristic of dry gas on  $\text{SnO}_2$ .

## Discussion

We have demonstrated that Sb(III) segregated to the surface of  $\text{SnO}_2$  forms an electrically active surface state which interacts with water. We have demonstrated an effect of this surface interaction upon the rate of the surface-catalyzed combustion of carbon monoxide.

Dramatic antimony segregation in  $\text{SnO}_2$  has previously been demonstrated by XPS<sup>11</sup> and it has been suggested<sup>32</sup> that, because not all the implanted Sb ions on the surface act as donor centers, Sb could also act as a trapping center. The mechanism for carrier trapping was supported by consideration of photoemission structure in the band gap region between valence and conduction bands.  $\text{SnO}_2$  thin films have shown<sup>33</sup> pronounced photoemission intensity above the main valence band structure

responsible for a shoulder that tails into the band gap region. Experiments performed on SnO<sub>2</sub>(110)<sup>34</sup> confirmed earlier suggestions<sup>28</sup> that this structure is to be associated with Sn ions at surface sites that trap a pair of electrons to become Sn(II) rather than Sn(IV). After implantation, the Sn(II) band gap structure was significantly attenuated (compare with Figure 4.). The evident changes in difference spectra suggest that antimony ions substitute for surface Sn ions, and electrons are then trapped into Sb<sup>3+</sup>-like surface states which lie at higher binding energy (BE) than the Sn<sup>2+</sup> states and overlap the main O 2p valence band intensity. Hence, the energy of the Sn(II) surface state is represented by a peak at 3 eV in the difference spectrum but it is not possible to observe the Sb(III) surface state energy directly in difference spectra.

A maximum Sb segregation was obtained at 800 °C for the 0.05% Sb-doped compounds (see Figure 3.). The enhancement in segregation with decrease of temperature corresponds to a heat of segregation  $\Delta H_{\text{seg}} \approx -20 \text{ kJ mol}^{-1}$ , consistent with the results in ref 11. The maximum is consistent with the assertion that, at the lowest reaction temperature, the product comprised a random array of disordered SnO<sub>6</sub> and SbO<sub>6</sub> octahedra,<sup>7</sup> rather than a solid solution of Sb in SnO<sub>2</sub>, so there would be no segregation. This assertion that at 600 °C firing the reaction to form a solid solution was incomplete, is sound because the valence band structure observed by XPS was almost indistinguishable from that of pure SnO<sub>2</sub>, and because the electrical conductivity of this material was almost identical to that of pure SnO<sub>2</sub> calcined at the same temperature. At higher calcination temperatures (1000 and 1200 °C) a decrease in Sb(III) concentration was observed, from the maximum obtained at 800 °C, which could be due to the diffusion of Sb<sup>3+</sup> into the bulk of the material. Our results on Sb surface segregation agree quantitatively with those of Cross and Pyke,<sup>11</sup> who showed that for calcination temperatures greater than 400 °C the surfaces became increasingly enriched in antimony, reaching a maximum for calcination temperature close to 1000 °C, with a surface enrichment factor of 7 with 4% atom of Sb and of 35 for 0.5% atom of Sb.

In the presence of gaseous oxygen, the elevated-temperature electrical conductivity of SnO<sub>2</sub> is determined by chemisorbed oxygen, trapping conduction electrons in surface states formulated as O<sub>2</sub><sup>-</sup>, O<sup>-</sup>, and O<sup>2-</sup>. Gas sensitivity of the electrical conductivity arises from changes in the surface concentration of these states.<sup>24</sup> Previous discussions starting from the observed square-root dependence of conductivity on concentration of reactive gas have particularly identified changes in the surface concentration of the O<sup>2-</sup> state as being responsible for the gas effects. Given this background, previous discussions<sup>24</sup> of the effect of water have postulated a transformation such as

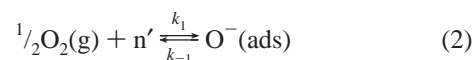


The trap state represented by OH<sub>ads</sub><sup>-</sup> is supposed to lie higher in the band gap than that represented by O<sup>2-</sup>, to account for the transformation causing an increase in conductivity. The expected effect of substitution of an electron donor into the lattice, giving an increase in conductivity, is to cause a decrease in the sensitivity to gases. Thus, the expected trend in the sensitivity to H<sub>2</sub>O, taking into account that the material calcined at 600 °C was essentially unreacted, is shown by the dashed line in Figure 5. Clearly, for a calcination temperature of 800 °C there was a significant enhancement of the electrical response to H<sub>2</sub>O, correlating with the segregation of Sb and the formation of the Sb(III) surface species. On these materials, the response to CO and CH<sub>4</sub>, dry, showed only effects attributable to the

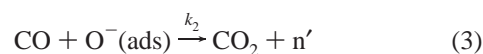
variation in particle size with calcination temperature (paper in preparation). Therefore, we have unequivocally demonstrated that the sensitivity to one chemical species (water) is specifically enhanced as a consequence of surface segregation changing the surface composition.

Sb(III) is a surface trap state for electrons.<sup>28</sup> The increase in conductivity caused by water adsorption could therefore be interpreted as water acting as an electron donor into this state. This is a molecular adsorption of H<sub>2</sub>O, rather than the dissociative adsorption postulated by eq 1. Sn(II)<sub>surf</sub> is also a surface trap for electrons, and the effect of water on undoped SnO<sub>2</sub> could, therefore, also be due to molecular adsorption onto the Sn(II) state. Later in this discussion we develop these ideas in more detail, proposing that the surface adsorption sites are best formulated as an association complex of an oxygen vacancy with Sn(II) or Sb(III).

Water vapor had a very strong effect on the surface-catalyzed oxidation of CO over doped and undoped SnO<sub>2</sub>. At a given temperature (e.g., 400 °C) the rate of combustion normalized to the surface area of all the materials for CO was greater under dry conditions than wet. However, the effect of Sb segregation was to cause a transition, over the temperature range of observation, from behavior characteristic of "wet" SnO<sub>2</sub> to that characteristic of "dry" SnO<sub>2</sub>. We can develop an interpretation which unifies the treatment of the electrical and the catalytic behavior by following the arguments advanced by Brown and Patterson.<sup>4</sup> These authors showed that the exchange of oxygen between the lattice and gaseous carbon dioxide or water was very rapid, even at room temperature, and that, in the oxidation of methane, the carbon dioxide formed incorporated equally oxygen derived from the lattice and oxygen adsorbed onto the surface from the gas. They showed that oxygen exchange between gas and lattice required much higher temperature, and that the reversible dissociative adsorption of oxygen contributed negligibly to this exchange. They postulated that surface oxygen vacancies mediated the oxygen exchange and that the catalytically active surface species was molecular oxygen adsorbed at reduced Sn sites. These ideas contrast with those put forward for the electrical behavior, which emphasize the importance of dissociative ionosorption of oxygen. Thus, to interpret the electrical behavior in the case of an n-type semiconducting oxide, such as SnO<sub>2</sub>, the chemistry taking place at the surface has been modeled by two main reactions. In the first reaction, atmospheric oxygen becomes chemisorbed to the surface consuming electrons



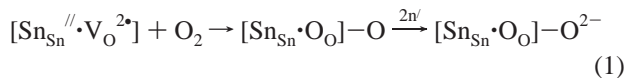
Reducing gases such as CO, present in the ambient air, produce a counter reaction



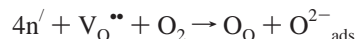
where n' is a conductance electron. The reducing gas removes the chemisorbed oxygen, frees up an electronic carrier, n', and raises the conductivity of the sensor. Analysis of the conductance variation with gas concentration implies that the active oxygen species is best formulated as O<sup>2-</sup>.<sup>24</sup> As noted before, the effects of water vapor have been discussed<sup>21,22,24</sup> in terms of the displacement of chemisorbed oxygen by H<sub>2</sub>O and OH<sup>-</sup>, producing, on SnO<sub>2</sub>, a surface electronic state such as a surface hydroxyl species, which lies higher in energy than the oxygen species which is displaced.

First, we postulate that a correct formulation of "adsorbed oxygen" is an oxygen molecule trapped in or on a surface oxygen vacancy. Following Brown and Patterson,<sup>4</sup> we propose that the combustion reaction proceeds partly through these species and partly through lattice oxygen at the surface. Then we propose that water competes with oxygen for the surface vacancies, blocking this route. This accounts for the diminution in the rate of the surface-catalyzed reaction in the presence of water. To account for the effect of antimony segregation on the reaction, we presume that the surface vacancy is correctly formulated as an association of Sn(II) with the vacancy in the absence of antimony, and of Sb(III) with the vacancy in the presence of surface-segregated antimony. Then we propose that the binding energy of water to the Sb(III)·V<sub>O</sub> surface defect complex is less than that to the Sn(II)·V<sub>O</sub> complex. The temperature variation of combustion rate would then correspond simply to the desorption of water from the defect complex. The apparent activation energy for combustion on the Sb-segregated sample would measure the heat of adsorption of water onto the surface defect.

Now we can make a connection between this interpretation and the electrical behavior. First, an elementary reaction between oxygen and a surface defect complex can be written:

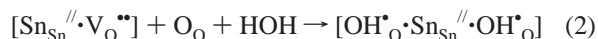


The overall stoichiometry of this reaction can be represented as



in which two electrons are trapped for each surface oxygen atom, as the interpretation of the electrical behavior requires. Interestingly, the mechanism as formulated here does not require dissociation of molecular oxygen.

A dissociative adsorption of water onto the surface defect complex is proposed:



In comparison with eq 1, the surface electron trap in eq 2 may lie at higher energy in the band gap, so replacement with water of oxygen adsorbed at the defect results in an increase of conductivity. Where Sb is surface segregated, the surface defect complex could be written [Sb<sub>Sb</sub><sup>3+</sup>·V<sub>O</sub><sup>••</sup>·Sb<sub>Sb</sub><sup>3+</sup>]. A similar formulation for the surface reactions can then be made. If the energy difference between OH state and oxygen state is bigger on this site, then the effect of water vapor on the conductivity would be larger. Such a statement is consistent with water being less strongly bound at this state than at the tin defect state represented in eq 2, and is thus consistent with the interpretation of the effect on combustion kinetics advanced above.

In summary, the study of the effect on electrical response and on combustion kinetics of Sb segregation in SnO<sub>2</sub> has

identified consequences linked to the adsorption of water. Discussion of these has suggested formulations for the surface defect states which mediate both the electrical behavior and the surface-catalyzed combustion.

**Acknowledgment.** We would like to thank the Engineering and Physical Sciences Research Council of the UK, Capteur Sensors and Analyzers Ltd., and the Ford Motor Company for financial support of this work.

## References and Notes

- Berry, F. J.; *Adv. Catal.* **1981**, *30*, 97.
- Weng, L. T.; Delmon, B. *Appl. Catal. A* **1992**, *81*, 141.
- McAteer, J.; *J. Chem. Soc., Faraday Trans. 1* **1979**, *75*, 2768.
- Brown, I.; Patterson, W. R.; *J. Chem. Soc., Faraday Trans. 1* **1983**, *79*, 1431.
- Caldararu, M.; Popa, V. T.; Sprinceana, D.; Ionescu, N. I. *Appl. Catal. A* **1995**, *125*, 247.
- Ono, T.; Yamanaka, T.; Kubokawa, Y.; Komiyama, M. *J. Catal.* **1988**, *109*, 423.
- Pyke, D. R.; Reid, R.; Tilley, R. J. D. *J. Chem. Soc., Faraday Trans. 1* **1980**, *76*, 1174.
- Volta, J. C.; Bussiere, P.; Coudurier, A.; Hermann, J. M.; Vedrine, J. C. *Appl. Catal.* **1985**, *16*, 315.
- Wakabayashi, K.; Kamiya, Y.; Ohta, H. *Bull. Chem. Soc. Jpn.* **1967**, *40*, 2172.
- Trimm, D. L.; Gabbay, D. S. *Trans. Faraday Soc.* **1971**, *67*, 2782.
- Cross, Y. M.; Pyke, D. R. *J. Catal.* **1979**, *58*, 61.
- Crozat, M.; Germain, J. E. *Bull. Soc. Chim. France* **1973**, *1*, 1125.
- Atkinson, L.; Day, P. *J. Chem. Soc. A* **1969**, 2423.
- Pyke, D. R.; Reid, R.; Tilley, R. J. D. *J. Solid State Chem.* **1978**, *25*, 1636.
- Orchard, A. F.; Thornton, G. *J. Chem. Soc., Dalton Trans.* **1977**, *13*, 1238.
- Marley, J. A.; Dockerty, R. K. *Phys. Rev.* **1965**, *140*, A304.
- Cox, P. A.; Egdell, R. G.; Orchard, A. F.; Harding, C.; Patterson, W. R.; Tavener, P. J. *Solid State Commun.* **1982**, *44*, 837.
- Hermann, J. M.; Portefaix, J. L.; Forissier, M.; Figueras, F.; Pichat, P. *J. Chem. Soc., Faraday Trans. 1* **1979**, *75*, 1346.
- Cox, P. A.; Egdell, R. G.; Flavell, W. R.; Kemp, J. P.; Potter, F. H.; Rastomjee, C. S. *J. Electron. Spectrosc.* **1990**, *54/55*, 1173.
- McAteer, J. F.; Moseley, P. T.; Norris, J. O. W.; Williams, D. E.; Tofield, B. C. *J. Chem. Soc., Faraday Trans. 1* **1987**, *83*, 1323.
- Morrison, S. R. *Sens. Actuators* **1982**, *2*, 329.
- Heiland, G. *Sens. Actuators* **1982**, *2*, 343.
- Yamazoe, N.; Fuchigami, J.; Kishikawa, M.; Seiyama, T. *Surf. Sci.* **1979**, *86*, 335.
- Williams, D. E. In *Solid State Gas Sensors*; Moseley, P. T., Tofield, B. C., Eds.; Adam Hilger: Bristol, 1987.
- Gercher, V. A.; Cox, D. F. *Surf. Sci.* **1995**, *322*, 177.
- Henrich, V. E.; Cox, P. A. *The Surface Science of Metal Oxides*; Cambridge University Press: Cambridge, 1994; p 316.
- Egdell, R. G.; Flavell, W. R.; Tavener, P. J. *J. Solid State Chem.* **1984**, *51*, 345.
- Cox, P. A.; Egdell, R. G.; Harding, C.; Patterson, W. R.; Tavener, P. J. *Surf. Sci.* **1982**, *123*, 179–203.
- Henshaw, G. S.; Gellman, L. J.; Williams, D. E. *J. Mater. Chem.* **1994**, *4*, 1427–1431.
- Wagner, C. D. In *Practical Surface Analysis*, 2nd ed.; Briggs, D.; Seah, M. P., eds.; Auger and X-ray Photoelectron Spectroscopy, Vol. 1; Wiley: Chichester, 1990; p 595.
- Williams, D. E.; Henshaw, G. S.; Pratt, K. F. E.; Peat, R. *J. Chem. Soc., Faraday Trans.* **1995**, *91(23)*, 4299–4307.
- Rastomjee, C. S.; Egdell, R. G.; Lee, M. J.; Tate, T. J. *Surf. Sci. Lett.* **1991**, *259*, L769.
- Rastomjee, C. S.; Egdell, R. G.; Georgiadis, G. C.; Lee, M. J.; Tate, T. J. *J. Mater. Chem.* **1992**, *2(5)*, 511.
- Themlin, J. M.; Sporken, R.; Darville, J.; Caudano, R.; Gilles, J. M.; Johnson, R. L. *Phys. Rev. B* **1990**, *42*, 11914.